ROBUST CONTROL AND MU-ANALYSIS OF A VEHICLE

Rakotovao N.H.[1], Randriamitantsoa P. A[2], Randriamitantsoa A. A[3]

[1] PhD student, Polytechnic University, University of Antananarivo, Antananarivo, Madagascar
[2] Professor Titular, Polytechnic University, University of Antananarivo, Antananarivo, Madagascar
[3] Professor, Polytechnic University, University of Antananarivo, Antananarivo, Madagascar

ABSTRACT

This document contributes to the control of a vehicle. More precisely, instead of a driver assistance system. Several studies have been developed in this direction, but we propose to develop a control system to assist the driver in turns, to respect the distance between two vehicles; avoid possible collisions; and a cruise control.

Keyword: - *Vehicle, H-infinity, Mu-analysis, fuzzy control, neural network*

1. INTRODUCTION

In this study, we will try to improve transportation safety, in particular to help reduce the risk of accidents in road travel. Since there are several themes related to this objective, we opted for the implementation of a driver assistance system to better value our study.

To do this, we will begin to implement an H-infinity control system for the models side (assistance for turning inputs) and longitudinal (vehicle tracking). Then, we will make a comparative study between the fuzzy controls and that of the neural network to determine a better speed regulator.

2. CONTROL OF A VEHICLE BY THE H-INFINITE METHOD

2.1. Lateral model control

Consider **Fig-1**. In order to set up a steering control system for driver assistance during cornering inputs, it is useful to use a dynamic model in which the state variables are in terms of error in position and orientation with respect to the road. Thus, the lateral model will be based on:

- V_y : lateral speed of the vehicle
- p : angular rate of roll
- ϕ : roll angle
- r : angular velocity of yaw

Hypothesis 01: Suppose our vehicle is traveling at a constant longitudinal speed V_x. And that it is perfectly symmetrical.

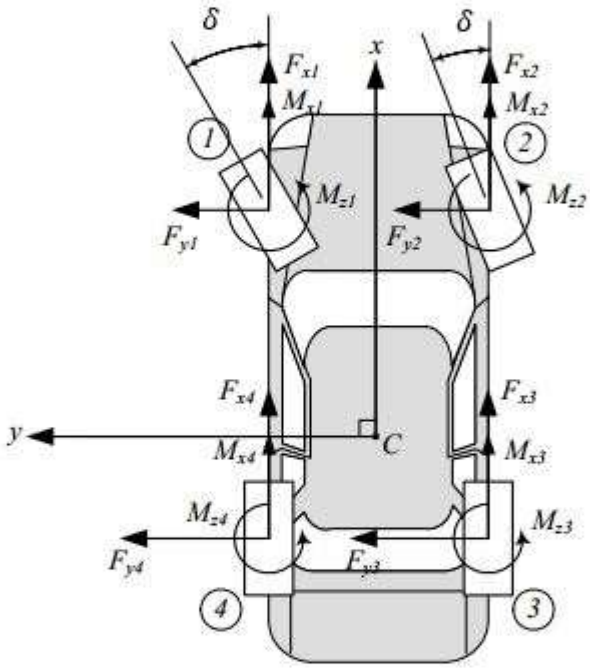

Fig -1 : Top view of a vehicle

With:

- F_{xav} : resulting from the longitudinal forces applied to the front wheels
- F_{xar} : resultant longitudinal forces applied to the rear wheels
- F_{yav} : resultant lateral forces applied to the front wheels
- F_{yar} : resultant lateral forces applied to the rear wheels
- M_x : moment in relation to the axis x
- M_z : moment in relation to the axis z
- δ : steering angle provided by the command

According to this hypothesis, the lateral model of the vehicle is given by:

$$\begin{cases} \dot{q} = Aq + B\delta \\ s = Cq + D\delta \end{cases} \qquad (01)$$

With:

$$q = \begin{bmatrix} V_y \\ p \\ \phi \\ r \end{bmatrix}$$

$$\dot{q} = \begin{bmatrix} \dot{V}_y \\ \dot{p} \\ \dot{\phi} \\ \dot{r} \end{bmatrix}$$

$$A = \begin{bmatrix} \frac{C_\beta}{mV_x} & \frac{C_p}{m} & \frac{C_\phi}{m} & \frac{C_r}{m} - V_x \\ \frac{E_\beta}{I_{xx}V_x} & \frac{E_p}{I_{xx}} & \frac{E_\phi}{I_{xx}} & \frac{E_r}{I_{xx}} \\ 0 & 1 & 0 & 0 \\ \frac{D_\beta}{I_{zz}V_x} & \frac{D_p}{I_{zz}} & \frac{D_\phi}{I_{zz}} & \frac{D_r}{I_{zz}} \end{bmatrix}$$

$$B = \begin{bmatrix} \frac{C_\delta}{m} \\ \frac{E_\delta}{I_{xx}} \\ 0 \\ \frac{D_\delta}{I_{zz}} \end{bmatrix}$$

$$C = \begin{bmatrix} 1 & 0 & 0 & 0 \\ 0 & 1 & 0 & 0 \\ 0 & 0 & 1 & 0 \\ 0 & 0 & 0 & 1 \end{bmatrix}$$

$$D = \begin{bmatrix} 0 \\ 0 \\ 0 \\ 0 \end{bmatrix}$$

The digital application allows us to obtain the following values:

$$A = \begin{bmatrix} -0{,}83 & -1{,}62 & 10{,}01 & -13{,}59 \\ 6{,}75 & -4{,}07 & -99{,}9 & -0{,}19 \\ 0 & 1 & 0 & 0 \\ -2{,}18 & -0{,}31 & 5{,}18 & -6{,}45 \end{bmatrix}$$

$$B = \begin{bmatrix} 62 \\ -69{,}33 \\ 0 \\ 32{,}11 \end{bmatrix}$$

The impulse response of the lateral model is given in **Fig-2**. It can be seen that the system is unstable since the impulse response is divergent.

The location of eigenvalues in the complex coordinate system (**Fig-3**) confirms this instability. The eigenvalues of the vehicle side model are shown in **Tab-1**. In order to stabilize the system, we determined a corrector using a classical synthesis method which is the solving of the standard problem by the Riccati matrix equations, known as the Glover-Doyle algorithm.

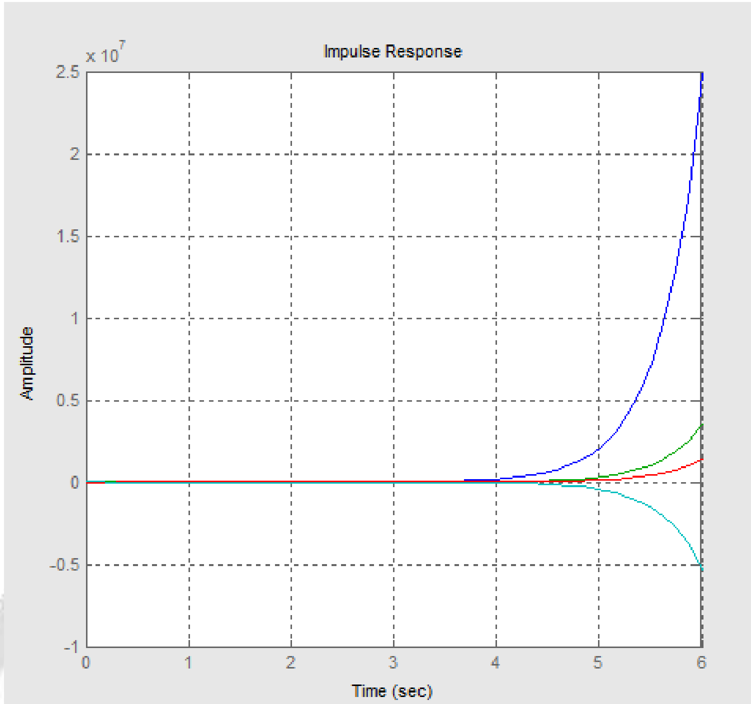

Fig -2 : Impulse response of vehicle steering speed

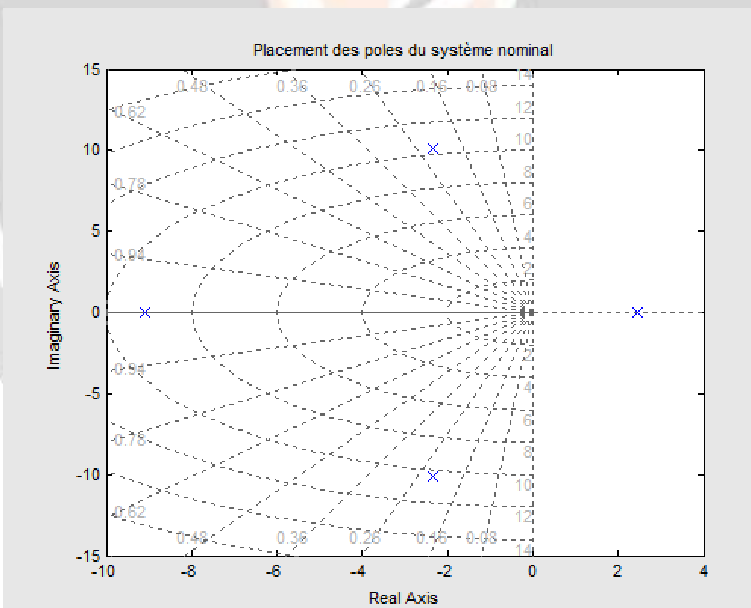

Fig -3 : Location of eigenvalues in a complex coordinate system

The corrector obtained by synthesis has the function of transfer:

$$K_{H0} = \begin{bmatrix} k1 \\ k2 \\ k3 \\ k4 \end{bmatrix} \qquad (02)$$

With:

- $k1 = \dfrac{3{,}996.10^5\ s^3 + 5{,}52.10^6 s^2 + 5{,}995.10^7\ s + 3{,}896.10^8}{s^4 + 1{,}642.10^5 s^3 - \ 1{,}414.10^6 s^2 + 5{,}164.10^7\ s - 9{,}492.10^8}$
- $k2 = \dfrac{0{,}5743.10^5\ s^3 + 0{,}7933.10^6 s^2 + 0{,}8617.10^7\ s + 0{,}56.10^8}{s^4 + 1{,}642.10^5 s^3 - \ 1{,}414.10^6 s^2 + 5{,}164.10^7\ s - 9{,}492.10^8}$
- $k3 = \dfrac{0{,}234.10^5\ s^3 + 0{,}3233.10^6 s^2 + 0{,}3511.10^7\ s + 0{,}2282.10^8}{s^4 + 1{,}642.10^5 s^3 - \ 1{,}414.10^6 s^2 + 5{,}164.10^7\ s - 9{,}492.10^8}$
- $k4 = \dfrac{-0{,}8624.10^5\ s^3 - 1{,}191.10^6 s^2 - 1{,}294.10^7\ s - 0{,}8409.10^8}{s^4 + 1{,}642.10^5 s^3 - \ 1{,}414.10^6 s^2 + 5{,}164.10^7\ s - 9{,}492.10^8}$

Table -1 : Own values of the vehicle side model

Real part	***Imaginary part***	***Frequency***	***Amortization***
2,45	0	-1	2,45
-2,36	10,1	0,228	10,4
-2,36	-10,1	0,228	10,4
-9,1	-6,16	1	9,1

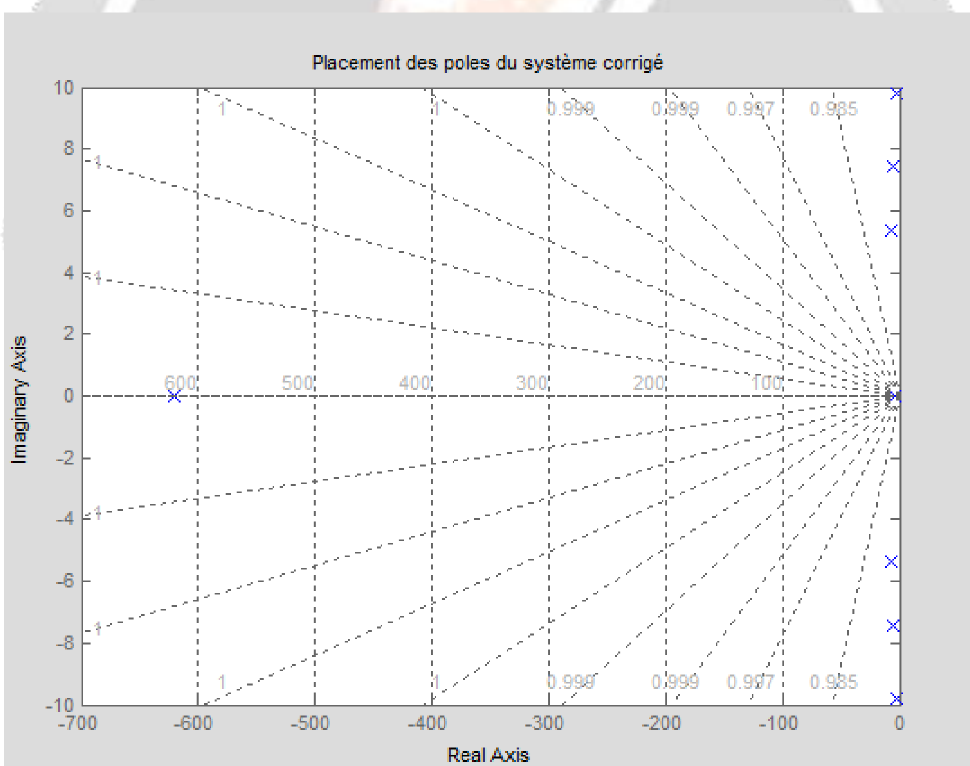

Fig -4 : Location of the eigenvalues of the corrected system in a complex coordinate system

Indeed, the corrector obtained is a vector of order 4 because the system has 4 outputs.

By applying the corrector to the system, **fig-4** shows that the corrected system is stable. Indeed, the poles of the corrected system have a negative real value. **Tab-2** also shows that all the poles have a real part less than -2.03 and that the complex poles have a damping lower than 1.

Table -2 : Own values of the lateral model of the vehicle (corrected)

Real part	***Imaginary part***	***Frequency***	***Amortization***
-4,48	0	4,48	1
-5,19	7,46	9,09	0,521
-5,19	-7,46	9,09	0,521
-7,40	5,38	9,15	0,809
-7,40	-5,38	9,15	0,809
-2,03	9,78	9,99	0,203
-2,03	-9,78	9,99	0,203
-620	0	6,20	1

As part of the nominal performance study, **Fig-5** represents the block diagram of the nominal performance. The weighting chosen has the transfer function:

$$w_1 = \frac{s+38}{s+36} \quad (03)$$

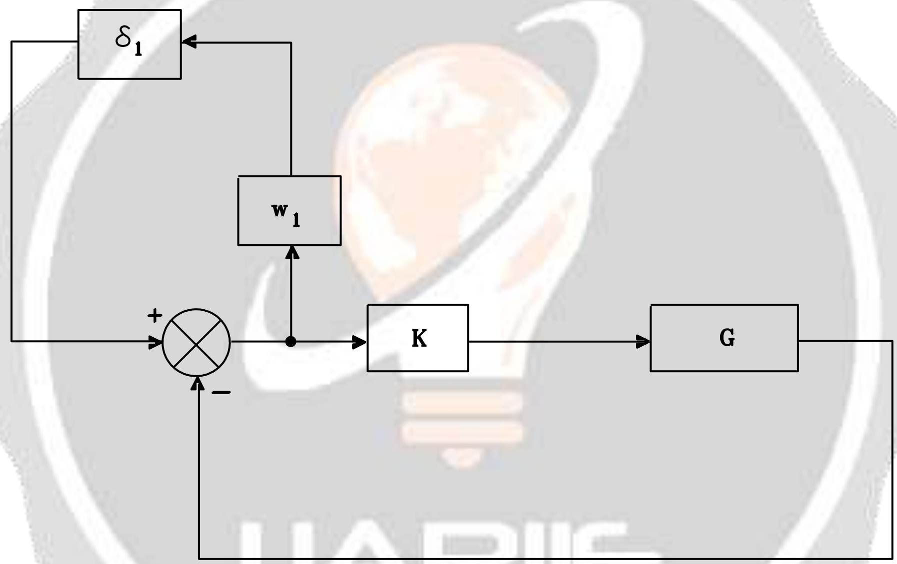

Fig -5 : Simulation diagram of nominal performance

The uncertainty matrix of the nominal performance is:

$$\Delta_{pn} = \{\delta_1 \in \mathbb{C}\} \quad (04)$$

By isolating the complex uncertainty Δ_{pn}, we obtain the analysis scheme of the nominal performance. (**Fig-6**)

Fig-7 shows the frequency responses of the sensitivity $S(j\omega)$, the complementary sensitivity function $T(j\omega)$ and the inverse of the weighting function.

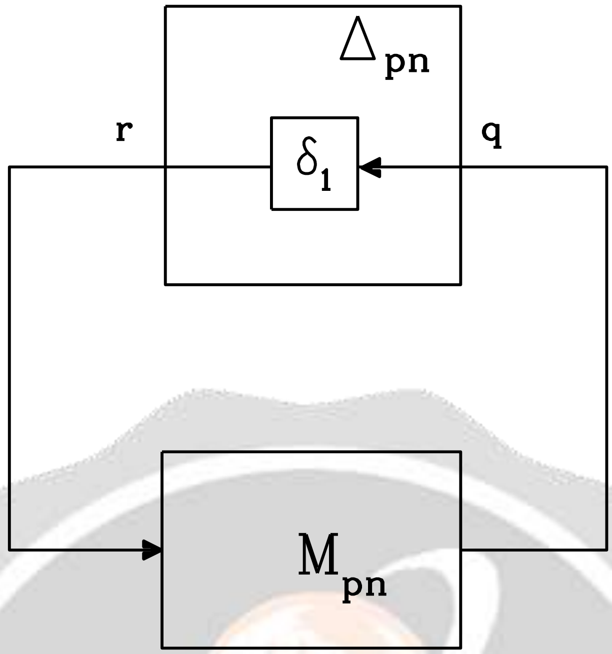

Fig -6 : Diagram of analysis of the nominal performance of the lateral model

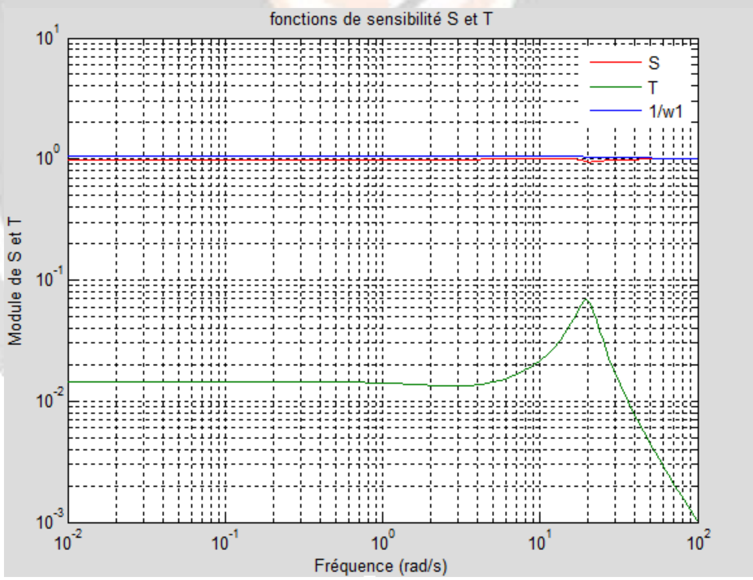

Fig -7 : Frequency responses of the sensitivity and complementary sound function (lateral model)

We observe that

$$|S(j\omega)| < \frac{1}{|w_1(j\omega)|} \tag{05}$$

The nominal performance condition is therefore verified.

2.2. Control of the longitudinal model

Consider a chain of vehicles on the road using a longitudinal control system for tracking vehicles. (**Fig-8**)

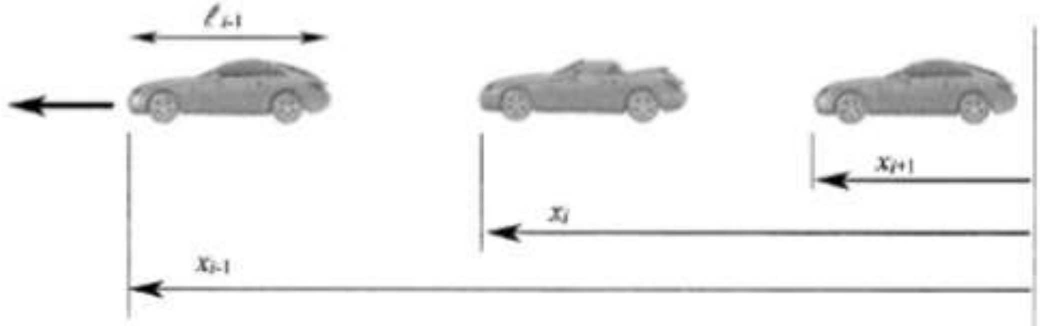

Fig -8 **:** Vehicle chain

We want our system to ensure the individual stability of the vehicle. Indeed, the control system is to control the spacing between two vehicles through the acceleration.

The transfer function for vehicle tracking is given by:

$$\frac{\delta_i}{\delta_{i-1}} = \frac{s+\lambda}{h\tau s^3 + hs^2 + (1+\lambda h)s + \lambda} \tag{09}$$

With:

- λ : time constant
- h : time interval
- τ : offset time between acceleration control and system response
- δ_i : spacing error for the $i\_ème$ vehicle

The digital application allows us to obtain equation 10.

$$G(s) = \frac{s+4}{0{,}225s^3 + 0{,}3s^2 + 2{,}2s + 4} \tag{10}$$

The impulse response of the longitudinal model is given in **Fig-9**.

It is found that the system is unstable since the impulse response is sinusoidal with increasing amplitude. The location of the eigenvalues in the complex coordinate system (**Fig-10**) confirms this instability. The eigenvalues of the longitudinal model of the vehicle are shown in **Tab-3**.

In order to stabilize the system, we used the same method as that of the lateral model. The corrector obtained by synthesis has the function of transfer:

$$K_{HOL} = \frac{-4{,}773.10^6 s^2 - 4{,}598.10^5\, s + 1{,}312.10^7}{s^3 + 4{,}725.10^6 s^2 + 4{,}772.10^7\, s1{,}236.10^8} \tag{11}$$

Indeed, the corrector obtained is not a vector because the system has only one output and one input.

By applying the corrector to the system, **Fig-11** shows that the corrected system is stable. Indeed, the poles of the corrected system have a negative real value. **Tab-4** also shows that all the poles have a real part less than -0.197 and that the complex poles have a damping lower than 1.

Table -3 : Own values of the longitudinal model of the vehicle

Real part	*Imaginary part*	*Amortization*	*Frequency*
0,187	3,22	-0,0579	3,23
0,187	-3,22	-0,0579	3,23
-1,71	0	1	1,71

Table -4 : Own values of the vehicle longitudinal model (corrected)

Real part	*Imaginary part*	*Frequency*	*Amortization*
-0,325	0	0,325	1
-0,398	0	0,398	1
-0,837	0,816	1,17	0,716
-0,837	-0,816	1,17	0,716
-0,197	0,197	2,78	0,708
-0,197	-0,197	2,78	0,708

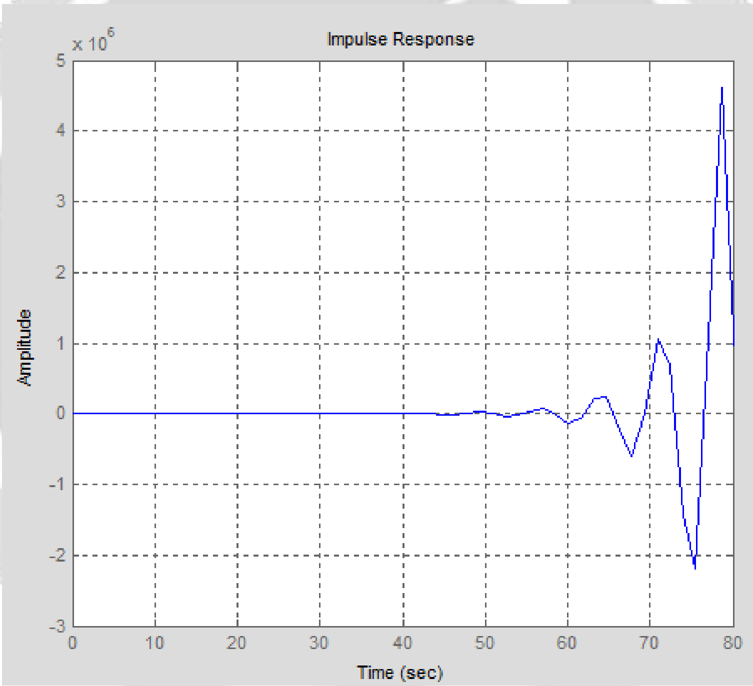

Fig -9 : Impulse response of the gap between two vehicles

For the study of the nominal performance, let us take again the **Fig-5** representing the block diagram for the study of the nominal performance.

The weighting chosen has the transfer function:

$$w_1 = \frac{s + 10{,}75}{s + 11} \tag{12}$$

We observe that

$$|S(j\omega)| < \frac{1}{|w_1(j\omega)|} \tag{13}$$

The nominal performance condition is therefore verified.

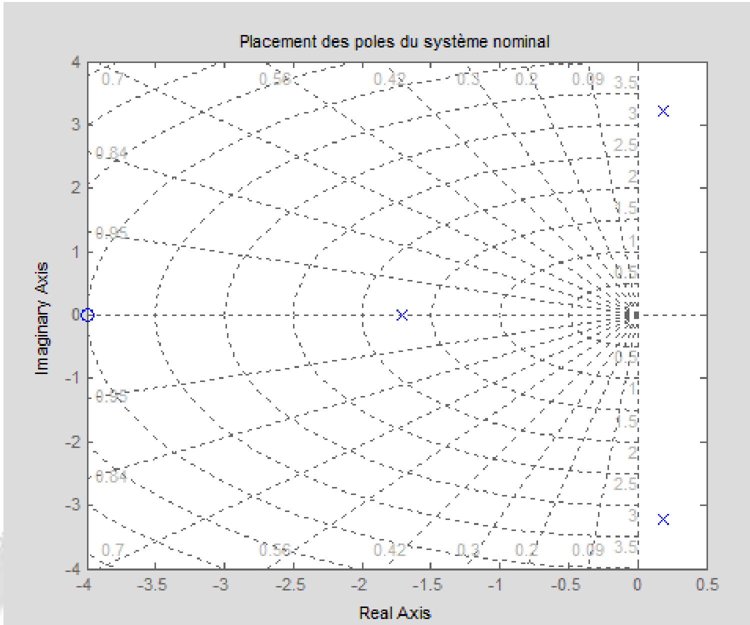

Fig -10 : Location of eigenvalues in a complex coordinate system

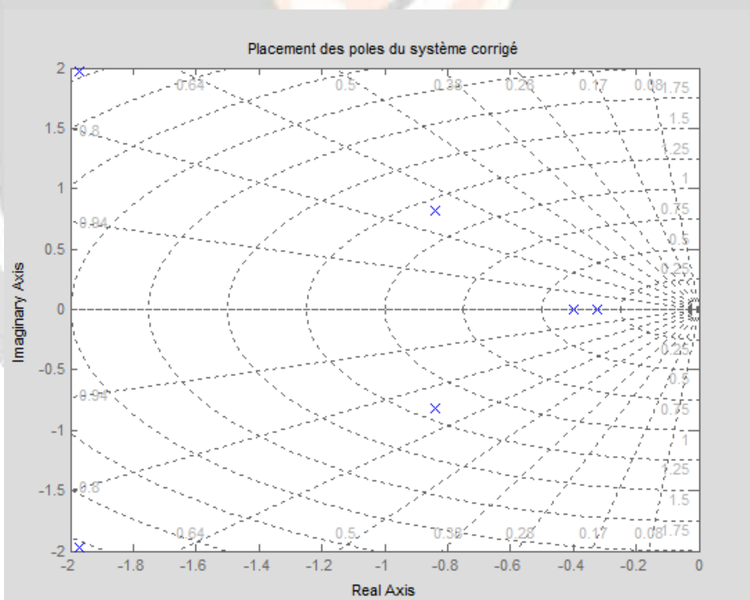

Fig -11 : Location of the eigenvalues of the corrected system in a complex coordinate system

Fig-12 shows the frequency responses of the sensitivity function $S(j\omega)$, the complementary sensitivity function $T(j\omega)$ and the inverse of the weighting function.

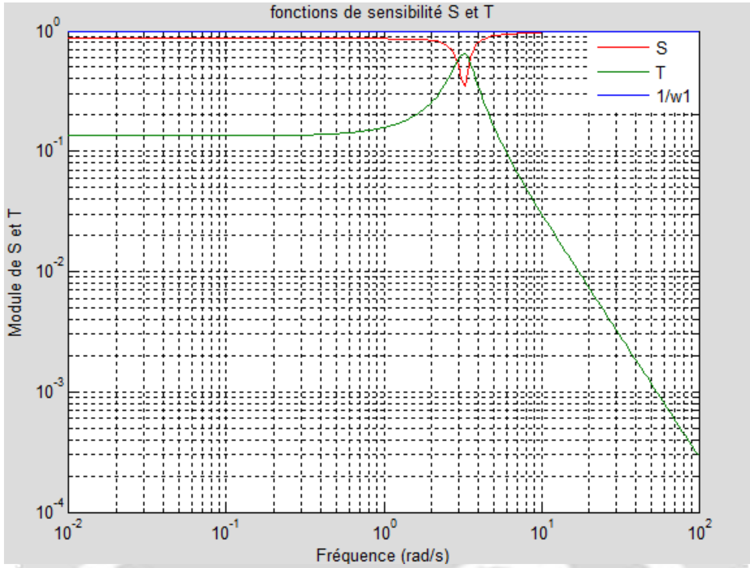

Fig -12 : Frequency responses of the sensitivity and complementary sound function (longitudinal model)

2.3. Control and analysis of the disturbed lateral model

For the rest, suppose that the parameters of the system are tainted with parametric uncertainty. Uncertain coefficients $\tilde{p}_i$ are modeled as follows.

$$\tilde{p}_i = p_i(1 + \omega_i\delta_i), |\delta_i| < 1 \quad (14)$$

With:

- p_i : nominal value of the parameter considered
- ω_i : corresponding weighting coefficient. $\omega_i = 0{,}2$

Applying the higher fractional linear transformation, equation 15 is then obtained:

$$\tilde{p}_i = [Q_{22} + Q_{21}\Delta_u(I - Q_{11}\Delta_u)^{-1}Q_{12}] \quad (15)$$

With:

$$Q_i = \begin{bmatrix} 0 & p_i \\ \omega_i & p_i \end{bmatrix}$$

In our model, we will assume that the lateral model of the vehicle is subject to two types of uncertainties:

- structured uncertainties on the coefficients of the rotation angle of the wheels (β) ;
- unstructured uncertainties.

We adopt a direct additive form model error for the synthesis our corrector. The weighting is chosen such that:

$$W_2 = \frac{s + 10}{2s + 50} \quad (16)$$

The corrector obtained by H-infinite synthesis has the function of transfer:

$$K_H = \begin{bmatrix} k1 \\ k2 \\ k3 \\ k4 \end{bmatrix} \quad (17)$$

With:

- $$k1 = \frac{4{,}044.10^{-5}\, s^4 - 26{,}88s^3 - 524{,}7s^2 - 5733s - 3{,}778.10^{-4}}{s^4 + 1{,}988.10^4 s^3 + 3{,}803.10^5 s^2 + 4{,}027.10^6\, s + 7{,}385.10^6}$$

- $$k2 = \frac{-4{,}589.10^{-4}\, s^4 + 30{,}5s^3 + 595{,}5s^2 + 6505s + 4{,}288.10^{-4}}{s^4 + 1{,}988.10^4 s^3 + 3{,}803.10^5 s^2 + 4{,}027.10^6\, s + 7{,}385.10^6}$$
- $$k3 = \frac{-1{,}969.10^{-7}\, s^4 + 0{,}1308\, s^3 + 2{,}554s^2 + 27{,}9s + 183}{s^4 + 1{,}988.10^4 s^3 + 3{,}803.10^5 s^2 + 4{,}027.10^6\, s + 7{,}385.10^6}$$
- $$k4 = \frac{2{,}202.10^{-5}\, s^4 - 14{,}64s^3 - 285{,}7s^2 - 3122s - 2{,}058.10^{-4}}{s^4 + 1{,}988.10^4 s^3 + 3{,}803.10^5 s^2 + 4{,}027.10^6\, s + 7{,}385.10^6}$$

By isolating the uncertainties δ_C, δ_D and δ_E of the parameter β we obtain the analysis diagram of the robustness in stability. (**Fig-13**)

The frequency response of the upper and lower bounds of the structured singular value of the stability analysis matrix of the system (M_{rs}) of the corrector is shown in **Fig-14**.

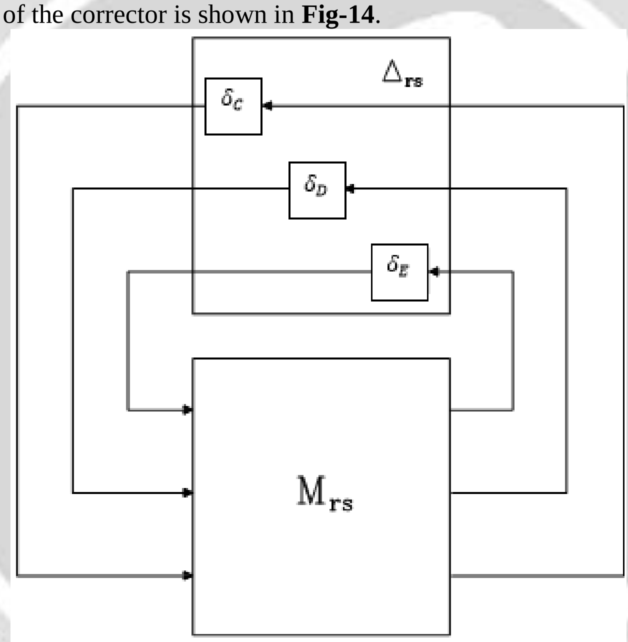

Fig -13 : Analysis diagram of the stability of the lateral model

The system is stable in robustness because $\max[\mu(M_{rs})] < 1$.

By isolating the uncertainties δ_1, δ_C, δ_D and δ_E , we obtain the stability analysis diagram shown in **Fig-15**.

The frequency response of the upper and lower bounds of the structured singular value of the stability analysis matrix of the system (M_{rp}) the corrector is represented by **Fig-16**.

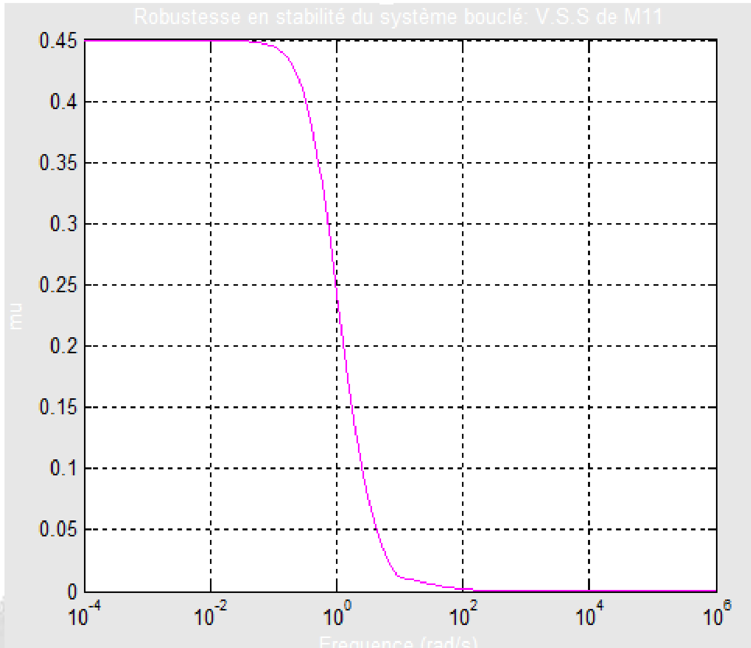

Fig -14 : Stability robustness analysis of the lateral model

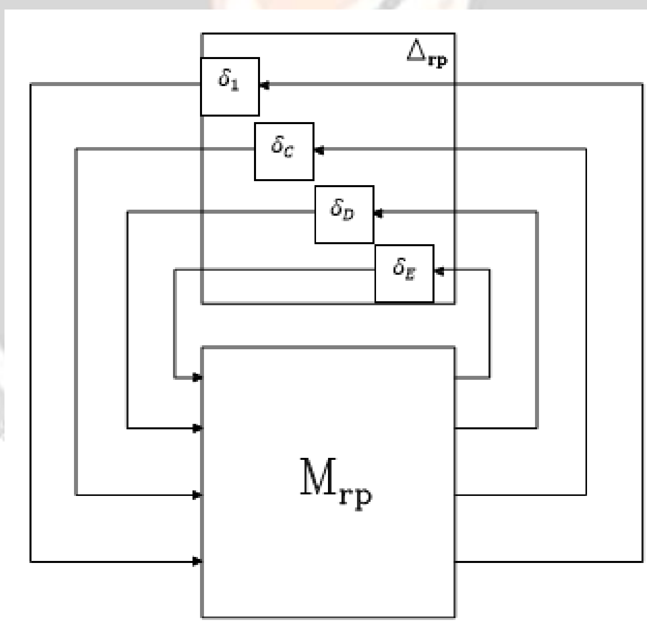

Fig -15 : Analysis diagram of the robustness in performance of the lateral model

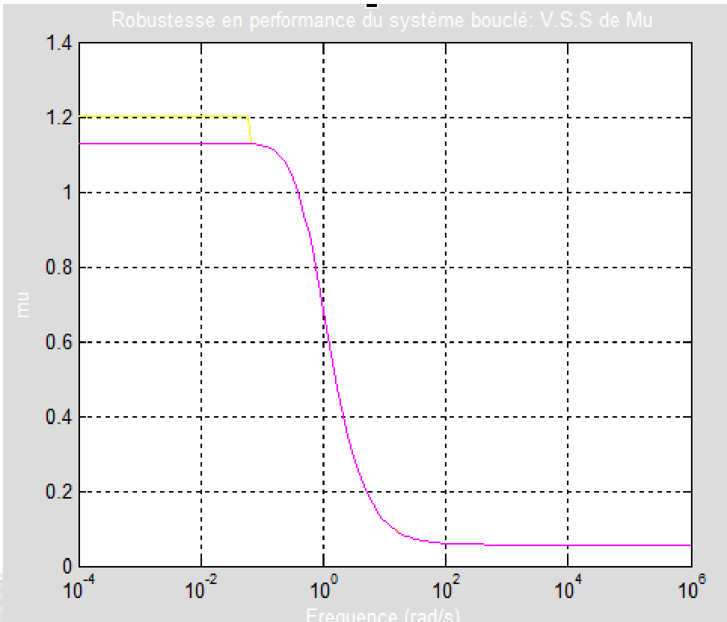

Fig -16 : Analysis of the robustness in performance of the lateral model

2.4. Control and analysis of the disturbed longitudinal model

For the longitudinal model, the system will be subject to two types of uncertainty:

- structured uncertainties on the coefficients λ, h and τ ;
- unstructured uncertainties.

The weighting is chosen such that:

$$W_2 = \frac{s + 10}{2s + 50} \tag{16}$$

The corrector obtained by H-infinite synthesis has the function of transfer:

$$K_{HL} = \frac{-7{,}286.10^{-5}\, s^3 + 0{,}08186\, s^2 + 0{,}1972\, s + 0{,}1309}{s^3 + 18{,}34 s^2 + 78{,}36 s + 147{,}8}$$

By isolating the uncertainties δ_λ, δ_h and δ_τ , we get the stability analysis schema in stability. (**Fig-17**)

The frequency response of the upper and lower bounds of the structured singular value of the stability analysis matrix of the system (M_{rs}) of the corrector is shown in **Fig-18**.

By isolating the uncertainties δ_1, δ_λ, δ_h and δ_τ , we obtain the analysis diagram of the robustness in performance. (**Fig-19**)

The frequency response of the lower and upper bounds of the structured singular value of the analysis matrix of the system performance robustness (M_{rp}) the corrector is shown in **Fig-20**.

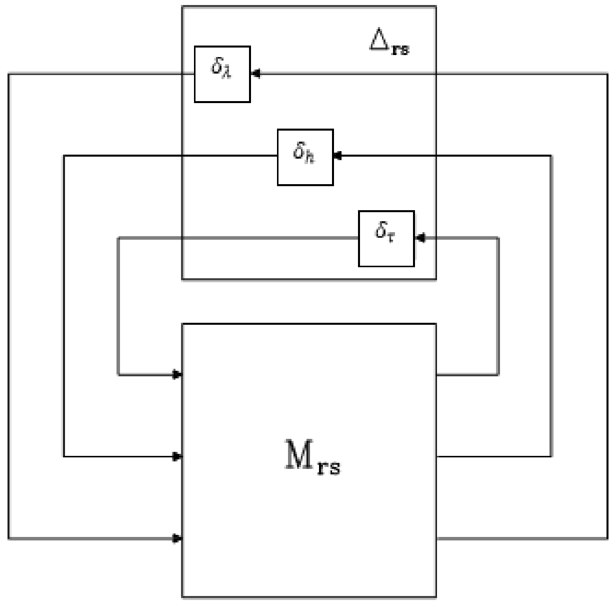

Fig -17 : Analysis diagram of the robustness in stability of the longitudinal model

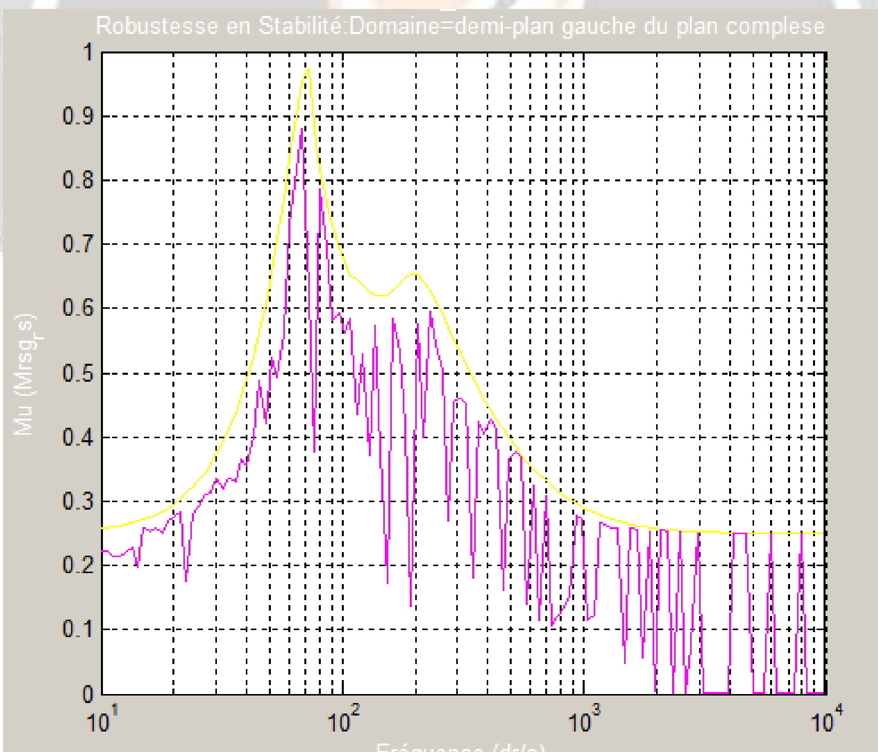

Fig -18 : Stability robustness analysis of the longitudinal model

The system is stable in robustness because $\max[\mu(M_{rs})] < 1$.

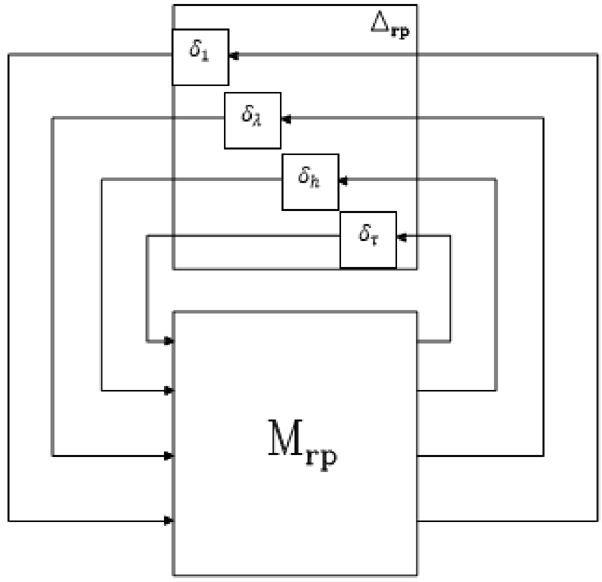

Fig -19 : Analysis diagram of the robustness in performance of the lateral model

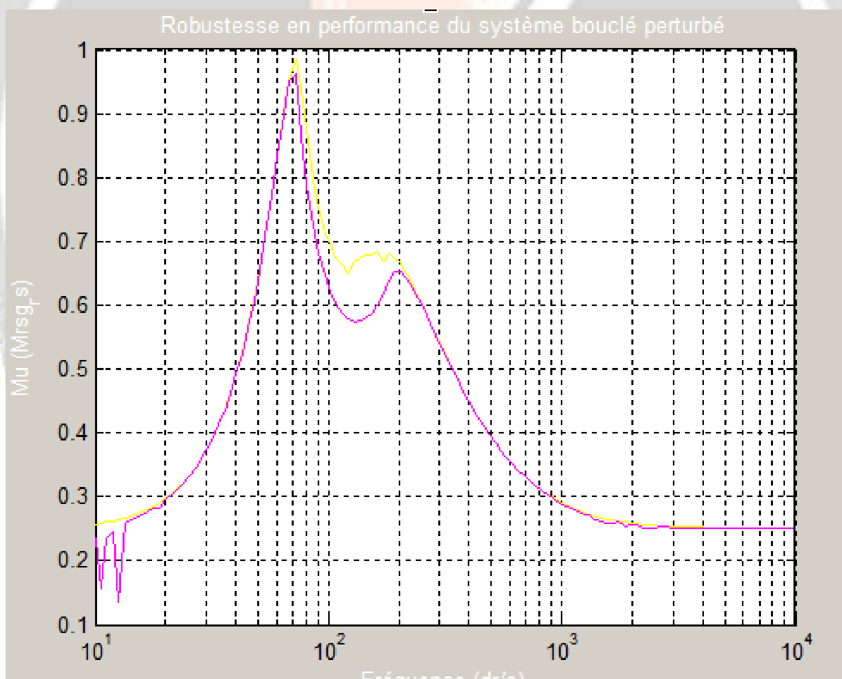

Fig -20 : Analysis of the robustness in performance of the lateral model

3. CRUISE CONTROL

We want the vehicle speed to be controlled to a desired value (80km / h) using the throttle control input. The cruise control of a vehicle can be modeled according to equation 17:

$$m\ddot{x} = \frac{T_e i_g}{r_{eff}\ R} - \frac{1}{2}\rho C_d A_F V^2 - mg\ (\sin(\theta) + cos(\theta)) \tag{17}$$

With:

- T_e : engine torque
- r_{eff} : effective radius of the rotating tire
- R : gear ratio of the transmission
- m : mass of the vehicle
- g : gravitational acceleration
- θ : tilt angle of the road
- $\frac{1}{2}\rho C_d A_F V^2$: aerodynamic drag force on a vehicle
- i_g : gear ratio

3.1. Cruise control by fuzzy logic

Our fuzzy controller has for entries:

- the error between the set speed and the speed produced by the system
- the variation of the speed

These two parameters will allow us to determine the torque provided by the engine needed to maintain the desired speed. The fuzzy rule surface is given by **Fig-21**.

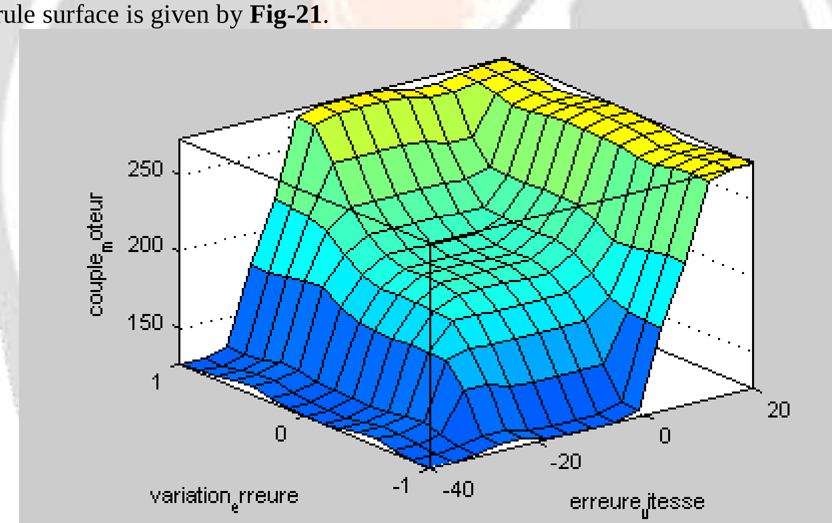

Fig -21 : Fuzzy rules base

After simulation, the result illustrated in **Fig- 22** was obtained.

The result of the simulation shows that the set speed is reached after $25min$ with a static error of $0{,}74\ km/h$

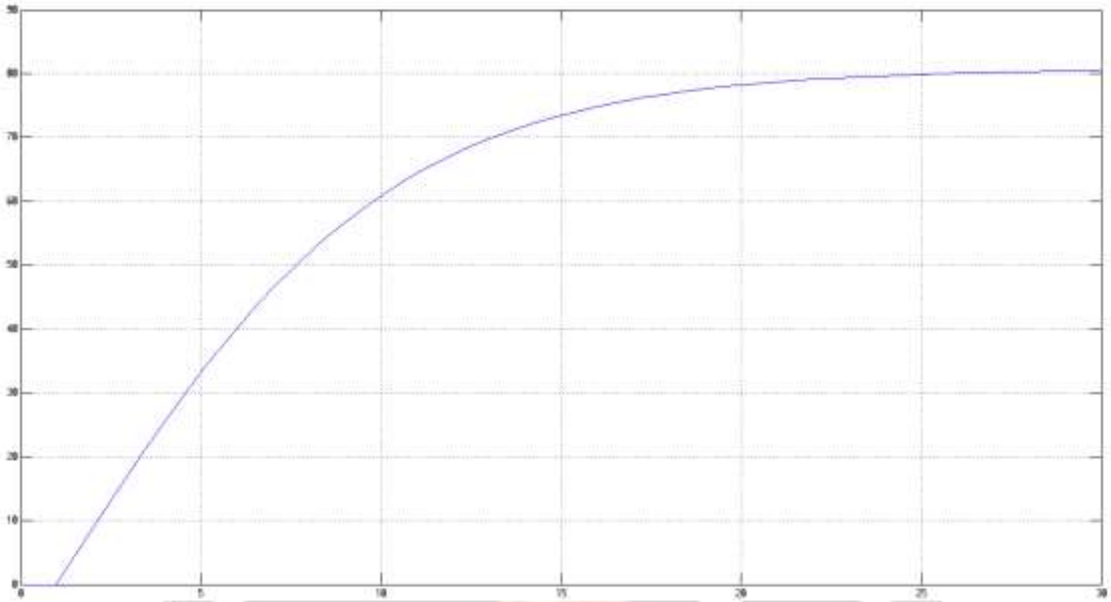

Fig -22 : Speed response subject to a fuzzy controller

3.2. Cruise control by the neuronal network

For this application, we will develop a reference control of the model. We chose a neuron network consisting of 10 hidden layers, 2 inputs and 2 outputs. The learning will be done after 300 Epoch and the method used is the retro propagation of Levenberg-Marquardt. After simulation, the result illustrated in **Fig-23**.This figure shows us that the set speed is reached after $28min$ and $45\ sec$ with a static error of $0{,}2\ km/h$. Thus, this type of corrector is more precise than the previous one, nothing less, slower.

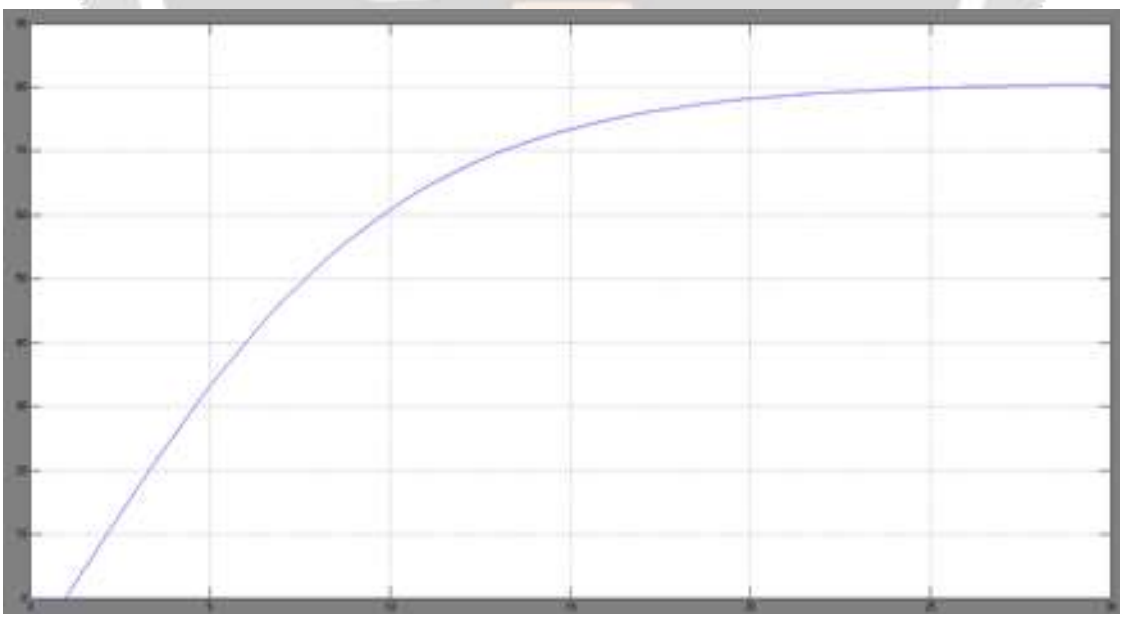

Fig -23 : Speed response subject to a neuronal network

4. CONCLUSION

This article contributes to improving safety in road transport. We were able to design a correction unit, using the H-infinity method, to assist the driver during cornering maneuvers and to maintain the inter-vehicle distance. During the analysis of the said correctors, we have found that they are both stable and efficient.

Speed regulation was performed by fuzzy control and neural network control. The comparative study allowed us to deduce that regulation by fuzzy control is faster but less precise than that of the neural network.

5. REFERENCES

[1]. RANARISON S.H *« Contribution à la modélisation, à la commande Robuste et à la Mu-analyse à temps continu d'un avion souple »*, Ecole Supérieure Polytechnique, 2018
[2]. RANDRIAMITANTSOA A.A *«Commande robuste et modélisation des systèmes informatiques d'un avion en vols longitudinal et latéral»*, Ecole Supérieure Polytechnique, 2013
[3]. Wuwei Chen *« Integrated vehicle dynamIcs and control »*,Wiley, 2016
[4]. Johannes Edelman *« Advanced Vehicle Control »* , Taylor&Francis, 2016